Framework for continuous quantification of spectral Coherence using Quadratic Time-Frequency distributions: exploring cardiovascular coupling

[1,2,3]Michele Orini, [1,2]Raquel Bailón, [1,2]Eduardo Gil, [3]Luca Mainardi and [1,2]Pablo Laguna
[1]Communications Technology Group, Aragón Institute of Engineering Research, University of Zaragoza, Zaragoza, Spain
[2]CIBER de Bioingeniería, Biomateriales y Nanomedicina (CIBER-BBN)
[3]Department of Biomedical Engineering, Politecnico di Milano, Italy

***Abstract*— Quadratic time-frequency (TF) distributions have an excellent joint TF resolution, but their applicability is limited by the presence of interferences. Interferences make a measure of TF coherence (TFC) based on these distributions inconsistent, unless a specific framework is set up to reduce their influence. In this communication, a framework for robustly estimating TFC, based on signal-dependent smoothing of the Wigner Ville distribution, is shown to provide a reliable continuous quantification of cardiorespiratory and cardiovascular interactions during non stationary conditions. Performance of the estimator is evaluated through a simulation example. Linear coupling between HRV and PTTV is then explored during segments of polysomnography recordings characterized by DAP episodes related to OSA. It is observed that when a DAP occurs TFC increases in LF range and decreases in HF range ($p < 0.05$).**

I. INTRODUCTION

Spectral coherence has been widely applied to quantify the strength of linear relationship between two signals. This measure, being defined in the frequency domain, can not assess the time evolution of the coupling between two signals and it is not appropriate for studying non stationary signals or transient phenomena. To assess the time evolution of linear coupling an extension of spectral coherence in time-frequency (TF) domain is necessary. In literature, multivariate parametric analysis has been proposed to continuously measure the mutual interaction between heart rate variability (HRV) and systolic blood pressure variability during tilting [1]. An other model based time-varying coherence function, able to estimate separately feedforward and feedback path of a close-loop, has been recently proposed and applied to explore the coupling of renal blood pressure and blood flow [2]. Parametric models are attractive because, thanks to their mathematical modeling, they provide a way to disentangle feedback and feedforward mechanisms, to identify systems also in close-loop conditions [3] and to evaluate the causal direction of a coupling [4]. Nevertheless, their performance in estimating the time varying spectral characteristics of a signal is related to the capability of fitting the appropriate underlying model and, in extremely non stationary conditions, they have been observed to perform less accurately than non parametric methods [5]. In a non parametric context, a measure of Time-Scale coherence, based on Continuous Wavelet Transform, has been recently applied to the study of cardiorespiratory interaction [6]. Non parametric methods have the advantage that they do not need any kind of assumption on the mathematical structure of the observed phenomenon and that they are relatively easy to estimate. Quadratic TF distribution represent a very powerful tool for the study of non stationary signals and transient phenomena and they have been widely applied to the study of autonomic nervous modulation [7]. Theoretical properties of TF coherence $\gamma(t,f)$ defined using quadratic distributions have been first described in [8] and [9], but, to our knowledge, it has never been used in biomedical applications. It is defined as:

$$\gamma(t,f) = \frac{C_{xy}(t,f)C^{*}_{xy}(t,f)}{C_{x}(t,f)C_{y}(t,f)} \tag{1}$$

where $C_{xy}(t,f)$ is the cross TF spectrum and $C_{x}(t,f)$ and $C_{y}(t,f)$ are the auto TF spectra, of signals $x(t)$ and $y(t)$, respectively. In [8] authors claim that choosing the positive distributions of the Cohen's class, the TFC in (1) maintains the desirable properties of the spectral coherence, in particular, it results to be bounded almost surely by unity (0 for totally uncorrelated signals and 1 for perfect linear correlation). In [9] it has been shown how (1) is properly bounded for jointly *underspread* processes, i.e. process $x(t)$ and $y(t)$ which do not have a widespread TF correlation. The main problem for the definition of a TFC based on quadratic distributions and bounded by unity is related to the presence of interference terms (ITs). Biological signals are often highly correlated in time and frequency (*overspread*) and a smoothing is needed to suppress ITs, but at detriment of joint TF resolution. The main purpose of this communication is to present an estimator for TF coherence based on signal-dependent quadratic TF representations and bounded to one in TF regions of interest. Its suitability for the continuous estimation of the interactions in cardiorespiratory and cardiovascular systems during non stationary conditions is discussed through a simulation study.

Real data application aiming at exploring the linear relationship between HRV and pulse transit time variability (PTTV) will be also presented. The high frequency component (HF, range [0.15-0.4] Hz) of the HRV signal is known to be strictly related to the parasympathetic system,

This work was partially supported by CIBER-BBN, by project TEC2007-68076-C02-02/TCM from MCyT and FEDER and by Grupo Consolidado GTC from DGA (Spain).

through respiratory sinus arrhythmia (RSA), while the low frequency component (LF,range [0.04-0.15] Hz) of the PTTV signal is thought to be directly affected by sympathetic vasoconstriction. The other two components (LF of HRV and HF of PTTV) are not that clearly related to an unique phenomenon. The quantification of the linear coupling between HRV and PTTV spectral components during a decrease in the amplitude fluctuations of photopletysmography (DAP), may provide useful information for better understanding how autonomic modulation is reflected in both signals.

II. METHODOLOGY

A. Quadratic Time-Frequency Distributions

The Wigner Ville distribution (WVD) is known to provide an excellent joint TF resolution. Unfortunately, the presence of ITs makes its applicability very limited. In order to reduce ITs, smoothed versions of the WVD, belonging to the Cohen's Class, have been proposed. Smoothing is performed as a 2D convolution between the WVD and a 2D kernel (defined in TF plane), which completely defines the properties of the distribution. Each distribution in the Cohen's Class can be interpreted as the 2D Fourier transform of a weighted version of the Ambiguity Function (AF) of the signal to be analyzed [10]. The cross-TF spectrum can be defined as:

$$\begin{aligned} C_{xy}(t,f;\phi) &= W_{xy}(t,f) **\phi(t,f) = \underset{\nu\to t}{\mathscr{F}_{\tau\to f}}\{A_{xy}(\nu,\tau)\Phi(\nu,\tau)\} \\ A_{xy}(\nu,\tau) &= \mathscr{F}_{t\to\nu}\left\{x(t+\frac{\tau}{2})y^{*}(t-\frac{\tau}{2})\right\} \\ \Phi(\nu,\tau) &= \underset{f\to\tau}{\mathscr{F}_{t\to\nu}}\{\phi(t,f)\} \end{aligned} \tag{2}$$

In (2) $**$ is the 2D convolution on t and f, $\mathscr{F}\{\cdot\}$ is the Fourier Transform operator and $A_{xy}(\nu,\tau)$ is the cross-AF of signals $x(t)$ and $y(t)$. The weighting (smoothing) function $\Phi(\nu,\tau)$ ($\phi(t,f)$) performs as a 2D low pass filter which should be tuned in order to find the better trade-off between ITs suppression and joint TF resolution (in TF domain) or, dually, between cross-component suppression and auto-terms concentration (in ambiguity domain). As the geometry of the kernel completely defines the performance of the TF distribution some efforts should be done toward the definition of versatile kernels, capable of automatically adjust to the TF structure of the signals being analyzed [11],[12]. Here, an elliptical exponential kernel is used:

$$\Phi(\nu,\tau;\nu_0,\tau_0,\lambda) = exp\left\{-\pi\left[\left(\frac{\nu}{\nu_0}\right)^2+\left(\frac{\tau}{\tau_0}\right)^2\right]^{2\lambda}\right\} \tag{3}$$

The kernel's iso-contours are ellipsis, ν_0 and τ_0 affect the length of the axes (the bandwidth of the 2D low pass filter) whereas λ sets its roll off.

B. The signal-dependent smoothing

Signals affected by the autonomic modulation may be modeled as the sum of complex exponentials showing both amplitude (AM) and frequency (FM) modulation, embedded in noise. In this study 2 exponentials are considered to model a AM LF and a AM-FM HF components:

$$x(t) = A_{LF}(t)e^{i\phi_{LF}(t)} + A_{HF}(t)e^{i\phi_{HF}(t)} + \xi(t) \tag{4}$$

where instantaneous frequency is $F(t) = (d\phi(t)/dt)/(2\pi)$. Quadratic TF distributions of these kinds of signals are expected to present both outer and inner ITs [13]. In order to suppress outer ITs, which mainly oscillate in time direction with a frequency which locally depends on the frequency lag $\nu_i = F_{HF} - F_{LF}$, the kernel should be able to filter out all $\nu > \nu_{i,min}$, where $\nu_{i,min}$ corresponds to the slowest ITs. To obtain $\nu_{i,min}$, the estimation of $F_{LF}(t)$ and $F_{HF}(t)$ is required. A direct or indirect estimation of respiratory rate can be used for approximating $F_{HF}(t)$. For the estimation of F_{LF}, which in the AF results to be concentrated along a line, the Hough Transform (HT) is applied to $|A(\nu,\tau)|$. Due to the hermitian symmetry of the AF, HT can be performed just on $(\nu,\tau) > 0$ resulting faster than in TF domain. The parameter ν_0 in (3) is fixed imposing that $\Phi(\nu_{i,min},0;\nu_0,\tau_0,\lambda) = k << 1$

$$\nu_0 = \nu_{i,min}\left(\frac{-log(k)}{\pi}\right)^{-\frac{1}{4\lambda}} \tag{5}$$

Given that, no information can help to retrieve the geometry of inner ITs, which mainly oscillate in frequency direction, in order to find the τ_0 providing a good compromise between inner ITs suppression and TF resolution, an iterative process is proposed. The parameter τ_0 is gradually reduced (increasing smoothing) until auto TF spectra are positive or, eventually $\gamma(t,f)$ is bounded to unity in the TF region of interest. Using the former criterion ($C_x(t,f) > 0$), the inner ITs are not completely removed, but their oscillations never take negative values. Figures 1a-1b represent the case of an insufficient smoothing. Outer ITs are still present at midway between the two components and, as expected, they are higher where the two signal spectral components are closer. In Fig. 1c -1d the TF map computed with the optimized ν_0 is shown. It is free from outer ITs but not from inner ones (see Fig. 1d around 0.3 Hz). Finally, in Fig. 1e-1f the τ_0 for $C_x(t,f) > 0$ is used.

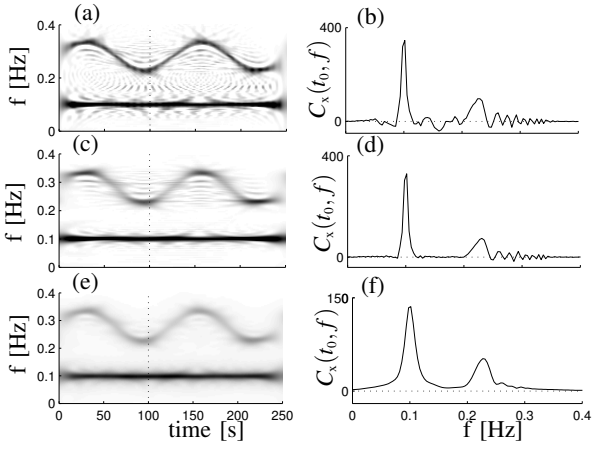

Fig. 1. Left: auto TF spectrum $C_x(t,f)$; $x(t)$ components are shown in Fig (2) and SNR=10dB; Right: $C_x(t_0,f)$, with t_0 marked by a dotted line in the left panels. (a)-(b): insufficient smoothing. (c)-(d): smoothing performed with a kernel optimized for outer ITs suppression. (e)-(f): smoothing performed with a kernel optimized for both outer and inner ITs attenuation.

C. Time-Frequency region of interest

The restriction of the TF support to a region of interest $\Omega(t,f)$ is justified by the desire of finding a good compromise between high joint TF resolution and boundness of $\gamma(t,f)$ by 1 (full suppression of ITs). The region of interest is then defined as the TF region $\Omega(t,f)$ where

$$\forall t, \quad C(t,f) > a \cdot \max_{f}[C(t,f)] \tag{6}$$

with $a<1$ and $\Omega(t,f) = \Omega_x(t,f) \cap \Omega_y(t,f)$. Once $\gamma(t,f)$ has been estimated, it is possible to track the time evolution of a single component coupling $\bar{\gamma}_{LF}(t)$ and $\bar{\gamma}_{HF}(t)$ by averaging $\gamma(t,f)$, defined in $\Omega(t,f)$, in LF and HF bands, respectively. In addition, a mean spectral coherence $\bar{\gamma}(f)$ (generally different from traditional spectral coherence) is retrieved averaging TFC on time. In those rare cases when, despite the positivity of both auto spectra, for some few points $(t_0,f_0) \in \Omega(t,f)$ $\gamma(t,f)>1$, the iterative process to compute τ_0 continues until the number of (t_0,f_0) is decreased to a very small, empirically determined, percentage of $\Omega(t,f)$ and the remaining (t_0,f_0) are excluded from $\Omega(t,f)$. In this way TF resolution and the consistency of the estimator can be both preserved. Those situations are due to inner interferences, which create small oscillations in the auto spectra which are not present in the cross-spectrum.

III. Materials

A. Simulation study

In a simulation study the model described in (4) is used to obtain 2 deterministic signals, $x(t)$ and $y(t)$, whose instantaneous frequencies and amplitudes are shown in Fig. 2. In both cases F_{LF} is constant and $F_{HF}(t)$ varies sinusoidally, which may model a situation of periodic breathing (abnormal respiration in which periods of shallow and deep breathing alternate). Amplitudes of $x(t)$ components are constant, whereas $A_{y,LF}(t)$ and $A_{y,HF}(t)$ linearly change in time. Note that $x(t)$ and $y(t)$ are coupled in LF band whereas no coupling is present in HF band. Moreover, in order to simulate a strong decorrelating event, during the interval T_ξ (see Fig. 2) $y(t)$ is replaced by a white noise with the same variance as $y(t)$. This abrupt change also introduces a very high amount of ITs in $C_y(t,f)$. One hundred pairs of signals, sampled at 4 Hz, have been created for SNR=20,10,5 dB and their TFC have been estimated.

B. Real data application

Real data application aims at exploring the linear relationship between HRV and PTTV (i.e. the time it takes a pulse wave to travel between two arterial sites) during DAP episodes related to obstructive sleep apnea (OSA). As detailed in [14], 175 selected signal segments centered around a strong DAP were extracted from complete night polysomnography recordings from 21 children (age 4.47±2.04). Pulse transit time was estimated as the interval between the peak of the R-wave on the ECG and the 50% peak value of the corresponding pulse in the finger pad measured by PPG. For every segment, the time evolution of the HRV-PTTV coupling in LF and HF band was extracted from the TFC.

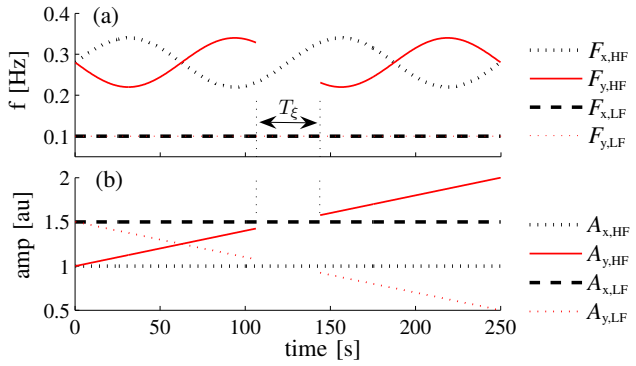

Fig. 2. Instantaneous frequencies (a) and amplitudes (b) of $x(t)$ and $y(t)$ used in the simulation study. In T_ξ $y(t)$ is replaced by a white noise.

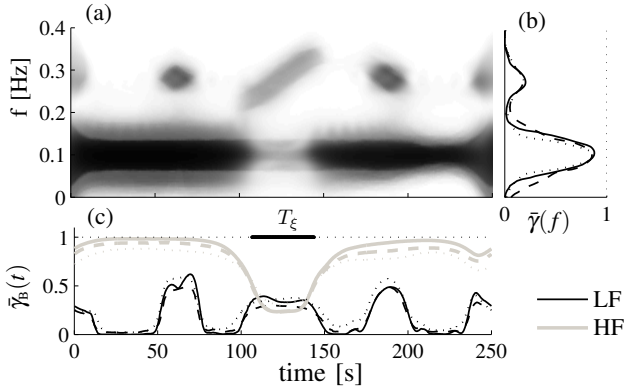

Fig. 3. (a): TFC, group average on 100 realization, between signals described in Fig 2 when SNR=10 dB. Color map goes from 0 (white) to 1 (black). (b) $\bar{\gamma}(f)$ is extracted from $\gamma(t,f)$ averaging TFC on time. (c) $\bar{\gamma}_B(t)$ is the trend of the coupling in B={LF,HF}. Continuous, dashed and dotted lines correspond to a SNR = 20, 10, 5 dB respectively. In T_ξ $y(t)$ is replaced by noise.

IV. Results and Discussion

A. Simulation study

Simulation results are shown in Fig. 3. The parameters ν_0 and τ_0 have been estimated as explained above, λ=0.25, k=0.002 and a=0.08. When positivity of the auto spectra was not sufficient to bound $\gamma(t,f)$, smoothing continues until reaching a quantities of not bounded points $< 0.2\%$ of $\Omega(t,f)$. Note that $\gamma(t,f)$ is high in LF band, except for the interval where noise replaces $y(t)$. The discontinuity introduced in T_ξ is detected with a good time resolution and, as expected, correlation decreases with noise. The thinning of $\Omega(t,f)$ observed in the latest part of the simulation (see Fig. 3a) is due to the contemporary increasing of $A_{y,HF}(t)$ and decreasing of $A_{y,LF}(t)$. Given that the points $(t_0,f_0) \notin \Omega(t,f)$ are not taken into account, the change in $\Omega(t,f)$ does not affect the estimation of $\bar{\gamma}_{LF}(t)$. In HF, TFC is always very low, excepted when $F_{x,HF}(t)$ and $F_{y,HF}(t)$ overlap (two gray spots around 60 and 200 s). The low but non zero values observed during T_ξ in HF band are due to the fact that the

TF region around $(T_\xi, F_{x,HF}(T_\xi)) \in \Omega(t,f)$. Note that the TFC estimator performs robustly even when SNR=5dB.

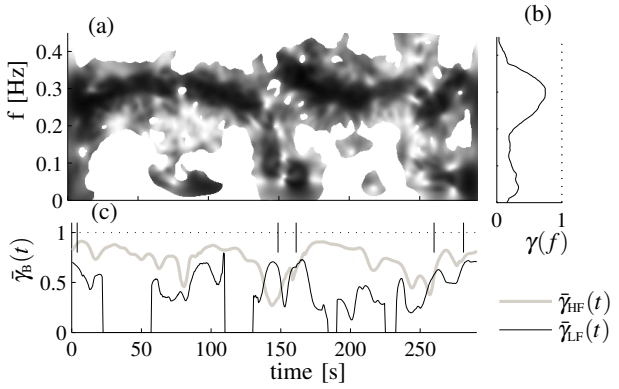

Fig. 4. (a):TFC map of one HRV-PTTV coupling. (b): $\bar{\gamma}_{LF}(t)$ and $\bar{\gamma}_{HF}(t)$ extracted from the TFC map. vertical lines marks DAP events

B. Real data application

The TFC map of HRV-PTTV coupling in one representative signal segment is shown in Fig. 4. The white regions in the TFC map in Fig. 4a represent the TF regions $\notin \Omega(t,f)$ where $\gamma(t,f)$ is not defined. When a DAP occurs (vertical lines) $\bar{\gamma}_{HF}(t)$ decreases while $\bar{\gamma}_{LF}(t)$ increases. In Fig. 5b the global $\bar{\gamma}^m_{LF}(t)$ and $\bar{\gamma}^m_{HF}(t)$ are represented as the median trends of all the 175 $\bar{\gamma}_{LF}(t)$ and $\bar{\gamma}_{HF}(t)$. The interquartile ranges of the median values of $\bar{\gamma}(t)$ estimated, for each signal segment, before (T_1), during (T_2) and after (T_3) the central DAP are plotted in Fig. 5*a*. Using both T-Student's test and Wilcoxon Test, the global increase of $\bar{\gamma}_{LF}(t)$ and the global decrease of $\bar{\gamma}_{HF}(t)$ during the central DAP result significant ($p < 0.05$). As shown in Fig. 4, the value of $\bar{\gamma}(T_1)$ and $\bar{\gamma}(T_3)$ is affected by the presence of other smaller DAPs. Analyzing separately the 26 signal segments with just one DAP, median values of $\bar{\gamma}_{HF}(T_1)$ and $\bar{\gamma}_{HF}(T_3)$ are observed to increase up to 0.9, while median values of $\bar{\gamma}_{LF}(T_1)$ and $\bar{\gamma}_{LF}(T_3)$ decrease to almost zero. Results support the idea that, in stable conditions, the respiratory component is equivalently represented in both HRV and PTTV, despite the fact that this oscillation has an autonomic origin in HRV and a mechanical one in PTTV. When a change in autonomic modulation occurs, its different origin is probably the main cause of $\bar{\gamma}_{HF}(t)$ reduction. Concerning the LF band, it has been noticed that a sympathetic activation tends to increase the PTTV-HRV coupling. This observation may support the idea that LF in HRV can be interpreted, at least in part, as a measure of sympathetic activation.

V. CONCLUSION

In this communication a framework for continuously quantifying the linear coupling of cardiovascular interactions using quadratic TF distributions has been presented. It represents an interesting tool for multivariate studies which aim at understanding how autonomic modulation is reflected in biomedical signals. This first application shows that in stable condition HRV and PTTV signals are correlated in respiratory frequency band while, during a DAP, their coherence decreases in HF band and it increases in LF band.

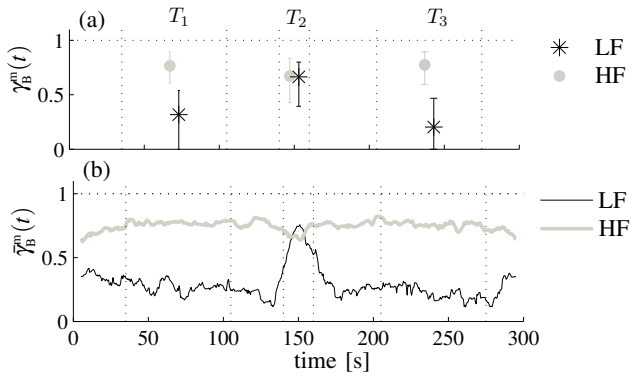

Fig. 5. (a) Interquartile range of all the median $\bar{\gamma}(T_1)$, $\bar{\gamma}(T_2)$ and $\bar{\gamma}(T_3)$. (b) Global time evolution of HRV-PTTV coupling in LF and HF range. DAP occurs in T_2

REFERENCES

[1] Mainardi and al., "Multivariate time-variant identification of cardiovascular variability signals: a beat-to-beat spectral parameter estimation in vasovagal syncope," *IEEE Trans. Biomed. Eng.*, vol. 44, no. 10, pp. 978–989, 1997.

[2] H. Zhao, W. A. Cupples, K. H. Ju, and K. H. Chon, "Time-varying causal coherence function and its application to renal blood pressure and blood flow data," *IEEE Trans. Biomed. Eng.*, vol. 54, no. 12, pp. 2142–2150, 2007.

[3] A. Porta, G. Baselli, and S. Cerutti, "Implicit and explicit model-based signal processing for the analysis of short-term cardiovascular interactions," *Proceedings of the IEEE*, vol. 94, no. 4, pp. 805–818, 2006.

[4] A. Porta and al., "Quantifying the strength of the linear causal coupling in closed loop interacting cardiovascular variability signals." *Biol Cybern*, vol. 86, no. 3, pp. 241–251, 2002.

[5] M. Orini, R. Bailón, P. Laguna, and L. T. Mainardi, "Modeling and estimation of time-varying heart rate variability during stress test by parametric and non parametric analysis," in *Proc. Computers in Cardiology*, 2007, pp. 29–32.

[6] K. Keissar, L. R. Davrath, and S. Akselrod, "Coherence analysis between respiration and heart rate variability using continuous wavelet transform," *Phil. Trans. R. Soc. A*, vol. 367, no. 1892, pp. 1393–1406, 2009.

[7] L. T. Mainardi, "On the quantification of heart rate variability spectral parameters using time-frequency and time-varying methods," *Phil. Trans. R. Soc. A*, vol. 367, no. 1887, pp. 255–275, 2009.

[8] L. B. White and B. Boashash, "Cross spectral analysis of nonstationary processes," *IEEE Trans. Inf. Theory*, vol. 36, no. 4, pp. 830–835, 1990.

[9] G. Matz and F. Hlawatsch, "Time-frequency coherence analysis of nonstationary random processes," in *Proc. Tenth IEEE Workshop on Statistical Signal and Array Processing*, 2000, pp. 554–558.

[10] F. Hlawatsch, "Duality and classification of bilinear time-frequency signal representations," *IEEE Trans. Signal Process.*, vol. 39, no. 7, pp. 1564–1574, 1991.

[11] R. G. Baraniuk and D. L. Jones, "A signal-dependent time-frequency representation: optimal kernel design," *IEEE Trans. Signal Process.*, vol. 41, no. 4, pp. 1589–1602, 1993.

[12] A. Costa and G. Boudreau-Bartels, "Design of time-frequency representations using a multiform, tiltable exponential kernel," *IEEE Trans. Signal Process.*, vol. 43, no. 10, pp. 2283–2301, 1995.

[13] F. P. Hlawatsch F, *The Wigner Distribution - theory and applications in signal processing*. Elsevier, 1997, pp. 59–113.

[14] E. Gil, M. Mendez, J. M. Vergara, S. Cerutti, A. M. Bianchi, and P. Laguna, "Discrimination of sleep apnea related decreases in the amplitude fluctuations of ppg signal in children by hrv analysis," *IEEE Trans. Biomed. Eng.*, in press.

Michele Orini,
Communications Technology Group, Zaragoza University
C/ Maria de Luna 1, 50018 Zaragoza, Spain
Tel: +34-976-76-27-04, Email: michele@unizar.es